

NACA TN 3735

# NATIONAL ADVISORY COMMITTEE FOR AERONAUTICS

TECHNICAL NOTE 3735

BENDING TESTS OF RING-STIFFENED CIRCULAR CYLINDERS

By James P. Peterson

Langley Aeronautical Laboratory  
Langley Field, Va.



Washington

July 1956

BENDING TESTS OF RING-STIFFENED CIRCULAR CYLINDERS

By James P. Peterson

SUMMARY

Twenty-five ring-stiffened circular cylinders were loaded to failure in bending. The results are presented in the form of design curves which are applicable to cylinders with heavy rings that fail as a result of local buckling.

INTRODUCTION

The ring-stiffened shell is efficient as an aircraft fuselage for transmitting bending or shear loads if the loading is large. For smaller loadings, a more efficient structure can be obtained by stabilizing the shell in some manner such as by the addition of stringers to the shell or by the use of waffle-like or sandwich-type plates for the shell. The bending and shear strength of these types of construction are not known to the desired degree of accuracy and the designer must usually supplement his existing knowledge on the subject with tests simulating the proposed design. Such a scheme rarely leads to the most efficient use of material and evidently suggests that more design data on fuselage construction are needed. In order to provide information on one phase of this problem, a series of bending tests on ring-stiffened circular cylinders was made at the Langley structures research laboratory. The main structural parameters varied in the tests were the ratio of ring spacing to radius and the radius-thickness ratio. The geometric size of the cylinders was also varied because the size has been suggested as a possible contributing factor in explaining the disparity between theory and experiment or the discrepancy between two test series. The rings used in the test series were heavy in order to eliminate general-instability-type failures which involve simultaneous failure of the cylinder wall and the rings.

The theoretical studies that have been made on the strength of the ring-stiffened shell in either bending or compression do not adequately predict its strength. Considerable progress has been made, however, which has clarified the importance of the various factors (load-shortening curve, initial eccentricities, and so forth) that are mainly responsible for the poor predictions (see, for example, refs. 1 and 2). Numerous experimental studies have been made, but, for the most part,

the studies were made on compression cylinders with large radius-thickness ratios and consequently are not in the range of loading where the ring-stiffened shell is efficient. Furthermore, these studies were made on one-bay cylinders clamped between heavy end fixtures. This type of specimen may be an unrealistic counterpart to the case of interest, the ring-stiffened shell.

### SYMBOLS

$l$	ring spacing, in.
$r$	radius of cylinder, in.
$t$	thickness of cylinder wall, in.
$E$	Young's modulus, ksi
$M_{cr}$	bending moment at cylinder buckling, in-kips
$M_f$	bending moment at cylinder failure, in-kips
$\mu$	Poisson's ratio
$\sigma_{cr}$	cylinder buckling stress, ksi

### TEST SPECIMENS AND TEST PROCEDURES

#### Test Specimens

A photograph of one of the cylinders ready for testing is shown in figure 1. The dimensions of the cylinders are given in table I. These dimensions are nominal except for those dimensions given for the wall thickness of the cylinders which represent the average of a large number of micrometer measurements. Dimensions of the rings used to stiffen the cylinders are given in figure 2. The location of the sheet splices on the compression side of the cylinders is indicated schematically in figure 3 where the upper half of the circle represents that part of the cylinder in compression. The cylinders had radius-thickness ratios  $r/t$  that varied from 120 to 750 and had ring-spacing-radius ratios  $l/r$  of  $1/4$ ,  $1/2$ , and 1 for most of the tests. For one value of  $r/t$  ( $r/t \approx 180$ ), additional cylinders with values of  $l/r$  of 2 and 4 were also tested.

The specimens were constructed of 7075-T6 aluminum alloy. Typical material properties were used in reducing the data. Young's modulus  $E$  was taken as 10,500 ksi and Poisson's ratio  $\mu$  was assumed to be 0.32.

### Test Procedures

Photographs of typical test setups are shown in figures 1 and 4. The loading frame in figure 1 was used when the expected failing moment was less than 3,000 inch-kips; otherwise the loading frame in figure 4 was used. The weight of end fixtures and that part of the test rig which would otherwise be supported by the test specimens was counter-balanced by weights to eliminate stray loads in the test specimens. The desired loads were applied to the loading frames by hydraulic jacks which were accurate to about 1 percent of the applied load.

When loading frames such as those shown in figures 1 and 4 are used, the load actually applied to the test specimen may be less than the indicated load at the jack because of friction in the bearings of the loading frame. In order to obtain a correction for this difference between indicated load and applied load, strains at a few locations on each of the cylinders were measured and compared with the strains expected to result from the indicated load. For the frame shown in figure 1, the mean error as measured by a large number of tests is 4 percent but the error may be as low as 1 percent or as high as 7 percent. The test results, as given later, have been corrected by 4 percent; therefore, the error in the results as presented, due to friction in the loading frame, may be as high as  $\pm 3$  percent. This method of adjusting the load for friction was used rather than relying solely on the measured strains because of the uncertainties that may beset any one test and cause local changes in the strain distribution from the expected elementary value. The number of tests made in the loading frame shown in figure 4 is much smaller, and the error due to friction has not been established as accurately as for the loading frame of figure 1. The few tests which have been made indicate that the error is much smaller and the results obtained by use of this frame have not been corrected for friction.

### TEST RESULTS

Values of the bending moments sustained by the test cylinders at buckling are given in table I. These moments represent the maximum moment as well as the buckling moment for those cylinders for which the bending moment at failure is not specifically tabulated. Values of the buckling stresses for the cylinders are given in table I and in figure 5 on a plot which has as ordinate and abscissa the parameters obtained by small-deflection theory (ref. 3). Also shown in figure 5 is a curve for

the buckling stress of cylinders in compression as given by small-deflection theory and several other curves which have been obtained by fairing lower limit curves to the present test data while using the theoretical curve as a guide.

On a plot such as used in figure 5, the theoretical curve has a slope of unity for values of the abscissa greater than about 10 and is given by the following familiar equation:

$$\sigma_{cr} = \frac{E}{\sqrt{3(1 - \mu^2)}} \frac{t}{r} \quad (1)$$

When data for a given radius-thickness ratio are parallel to this theoretical curve, the effect of ring spacing on the buckling stress is negligible. A study of the data as plotted in figure 5, or as given in table I, indicates that there is some gain in strength as the ring spacing is decreased but the gain is negligible until a value of  $l/r$  of  $1/2$  has been reached.

In constructing the empirical curves of figure 5, the curves were drawn parallel to the theoretical curve for values of the abscissa greater than that value corresponding to a cylinder with a ring-spacing-radius ratio of about  $1/2$ . The location of curves in this range was determined by plotting that part of the data from table I which was obtained from cylinders with a ring-spacing-radius ratio greater than about  $1/2$  on a logarithmic plot of  $\sigma_{cr}/E$  against  $r/t$  and then by fitting a straight lower limit line to the data (see fig. 6). For smaller values of the abscissa in figure 5, the curves are faired in to meet the theoretical curve for a compression cylinder simply supported at the rings. The trend of the data suggests that a more appropriate fairing of the empirical curves might be obtained by fairing into the theoretical curve for cylinders clamped at the rings instead of the curve for cylinders simply supported at the rings. However, the test cylinders had heavier rings and therefore a greater clamping action at the rings than is usually found in aircraft structures, and it is believed that the test data in this range of figure 5 are influenced by the clamping of the heavy rings.

A photograph of one of the cylinders after being tested to failure is shown in figure 7. The type of buckling exhibited is characteristic of that expected for cylinders with small values of the parameter  $\frac{l^2}{rt} \sqrt{1 - \mu^2}$ . For larger values of the parameter  $\frac{l^2}{rt} \sqrt{1 - \mu^2}$ , the buckle pattern for the test cylinders was the more familiar type of buckle characterized by successive in-and-out buckles along and around the cylinder.

## DISCUSSION OF RESULTS

One of the factors often mentioned when discussing discrepancies between test data from various investigators is the geometric size of the specimens (see, for instance, refs. 4 and 5). In order to study this effect, the geometric size was included as one of the variables in the present test series. Most of the data presented in figure 5 were obtained on cylinders with a diameter of about 30 inches (30-inch cylinders), but a few tests were made on 19-inch, 48-inch, and 77-inch cylinders as well. A comparison of the data from cylinders of various diameters (fig. 5) indicates that any size effect that exists must be small and is hidden because of the relatively large scatter in data from bending tests on cylinders of the same diameter.

The factor usually cited as being mainly responsible for the large disparity between theory and test for cylinders in compression or bending is initial imperfections or eccentricities. No attempt was made to determine the extent of initial eccentricities in the present test series except to lay a straight edge along the length of the cylinders in the process of inspecting the cylinders prior to testing. The specimens generally exhibited an appearance characteristic of good workmanship. However, the sheet splices, which run lengthwise in the cylinders, usually were bowed in slightly between rings. It is probable that this phenomenon is a result of "pounding out" the sheet in the neighborhood of the splice in the process of bucking the rivets, thereby creating an excess of surface area in this vicinity. The effect was considerably more pronounced on cylinders with thick skins and large ring spacings, and, on cylinder 25, the sheet splice bowed in about  $\frac{3}{16}$  inch between rings. When this cylinder was tested, the eccentricity grew slightly with load, and, when the moment reached about 2,600 inch-kips, the wall of the cylinder at the eccentricity snapped gently inward to form a buckle. The load was released and a  $1 \times 1\frac{1}{2} \times 1 \times \frac{3}{16}$  inch Z-section stringer was riveted along each of the four sheet splices in order to pull the splices out and remove the eccentricity. The cylinder was retested and, this time, sustained a moment of 4,465 inch-kips before buckling. The four stringers added about 1,500 inches<sup>4</sup> to the moment of inertia of the cylinder (which is less than 10 percent of the original moment of inertia) but were far enough apart circumferentially to have a negligible effect on the local buckling stress other than to remove the initial eccentricity. This type of eccentricity can be eliminated in design without appreciable loss in efficiency by the addition of stringers at sheet splices on the compression side of the fuselage or by eliminating sheet splices on the compression side of the fuselage. The latter can be accomplished for large fuselages by using the with-grain direction of the sheet in the circumferential direction of the fuselage.

Experimentally determined curves similar to those given in figure 5 have been published at various times summarizing available data for cylinders tested in compression (see refs. 3, 4, and 5). The object of such summaries is to provide design data for fuselages subjected to bending loads, but data from bending tests are not used because not much data of this type exist. A cylinder in bending can sustain an extreme fiber stress which is somewhat greater than the average stress obtainable in a similar cylinder tested in compression. By using theoretical considerations, Timoshenko (ref. 6) predicts a value of about 1.3 as the ratio of the buckling stresses for the two loading cases. Ratios from 1.3 to 1.8 were obtained in reference 7 in an experimental investigation. The curves of figure 5 give buckling stresses as much as two times the buckling stresses given by the corresponding curves of references 3 to 5 but were obtained from data on a different type of structure as well as for a different loading condition. The test specimens in the present investigation were ring-stiffened cylinders which had a short buffer bay on either end of the test section to help distribute the load in the neighborhood of the ends of the test section (see fig. 4). The one-bay type of specimens used previously does not have this characteristic and may have stress distributions in the neighborhood of the ends of the cylinders which are rather irregular and which may cause premature local buckling. The curves of figure 5 are believed, therefore, to be suitable for the prediction of the bending strength of ring-stiffened circular cylinders in which the rings are heavy enough so that general-instability-type failures do not occur.

#### CONCLUDING REMARKS

Design curves for ring-stiffened circular cylinders subjected to bending are given. The curves are based on test results from 25 cylinders with heavy rings in which failure was by local instability (between rings) rather than by general instability which involves simultaneous failure of the cylinder wall and rings. The design curves generally predict higher failing stresses than curves now in use which are based on tests of one-bay compression cylinders.

Langley Aeronautical Laboratory,  
National Advisory Committee for Aeronautics,  
Langley Field, Va., April 26, 1956.

## REFERENCES

1. Von Kármán, Theodore, and Tsien, Hsue-Shen: The Buckling of Thin Cylindrical Shells Under Axial Compression. Jour. Aero. Sci., vol. 8, no. 8, June 1941, pp. 303-312.
2. Donnell, L. H., and Wan, C. C.: Effect of Imperfections on Buckling of Thin Cylinders and Columns Under Axial Compression. Jour. Appl. Mech., vol. 17, no. 1, Mar. 1950, pp. 73-83.
3. Batdorf, S. B., Schilderout, Murry, and Stein, Manuel: Critical Stress of Thin-Walled Cylinders in Axial Compression. NACA Rep. 887, 1947. (Supersedes NACA TN 1343.)
4. Kanemitsu, Sunao, and Nojima, Noble M.: Axial Compression Test of Thin Circular Cylinders. Calif. Inst. Tech., Thesis, 1939.
5. Shelley, J. H.: Strength Data on Circular Metal Cylinders Under Axial Compression. Tech. Note No. Structures 122, British R.A.E., Aug. 1953.
6. Timoshenko, S.: Theory of Elastic Stability. McGraw-Hill Book Co., Inc., 1936, pp. 463-467.
7. Lundquist, Eugene E.: Strength Tests of Thin-Walled Duralumin Cylinders in Pure Bending. NACA TN 479, 1933.



TABLE I  
DIMENSIONS AND TEST RESULTS OF CYLINDERS

Cylinder	2r, in.	t, in.	l, in.	Test length, bays	M <sub>cr</sub> , in-kips	σ <sub>cr</sub> , ksi
1	19.16	0.0320	2.38	6	<sup>a</sup> 252	27.4
2	19.16	.0321	4.75	3	153	16.5
3	19.16	.0332	9.50	3	167	17.4
4	30.03	.0318	3.75	6	<sup>b</sup> 221	9.82
5	30.03	.0316	7.50	3	202	9.05
6	30.03	.0314	15.0	3	186	8.35
7	30.43	.0512	3.75	6	824	22.2
8	30.05	.0512	7.50	3	645	17.8
9	30.43	.0522	15.0	3	685	18.0
10	30.46	.0830	3.75	6	2,320	40.0
11	30.08	.0837	7.50	3	1,680	28.3
12	30.46	.0830	15.0	3	1,830	30.1
13	30.46	.0825	30.0	3	1,820	30.4
14	30.46	.0770	60.0	1	1,560	27.8
15	30.50	.127	7.50	3	4,535	49.2
16	30.50	.126	15.0	3	4,315	47.0
17	48.41	.0327	6.00	6	<sup>c</sup> 340	5.65
18	48.41	.0324	12.0	3	392	6.55
19	48.41	.0323	24.0	3	296	4.97
20	48.43	.0520	6.00	6	<sup>d</sup> 1,030	10.8
21	48.43	.0520	12.0	3	1,030	10.8
22	48.43	.0525	24.0	3	1,010	10.5
23	77.21	.0871	9.50	6	6,235	15.3
24	77.21	.0901	19.0	3	4,785	11.3
25	77.21	.0900	38.0	3	<sup>e</sup> 4,465	9.68

<sup>a</sup> M<sub>F</sub> = 254.

<sup>b</sup> M<sub>F</sub> = 288.

<sup>c</sup> M<sub>F</sub> = 455.

<sup>d</sup> M<sub>F</sub> = 1,260.

<sup>e</sup> Includes moment carried by four stringers. See text for details.

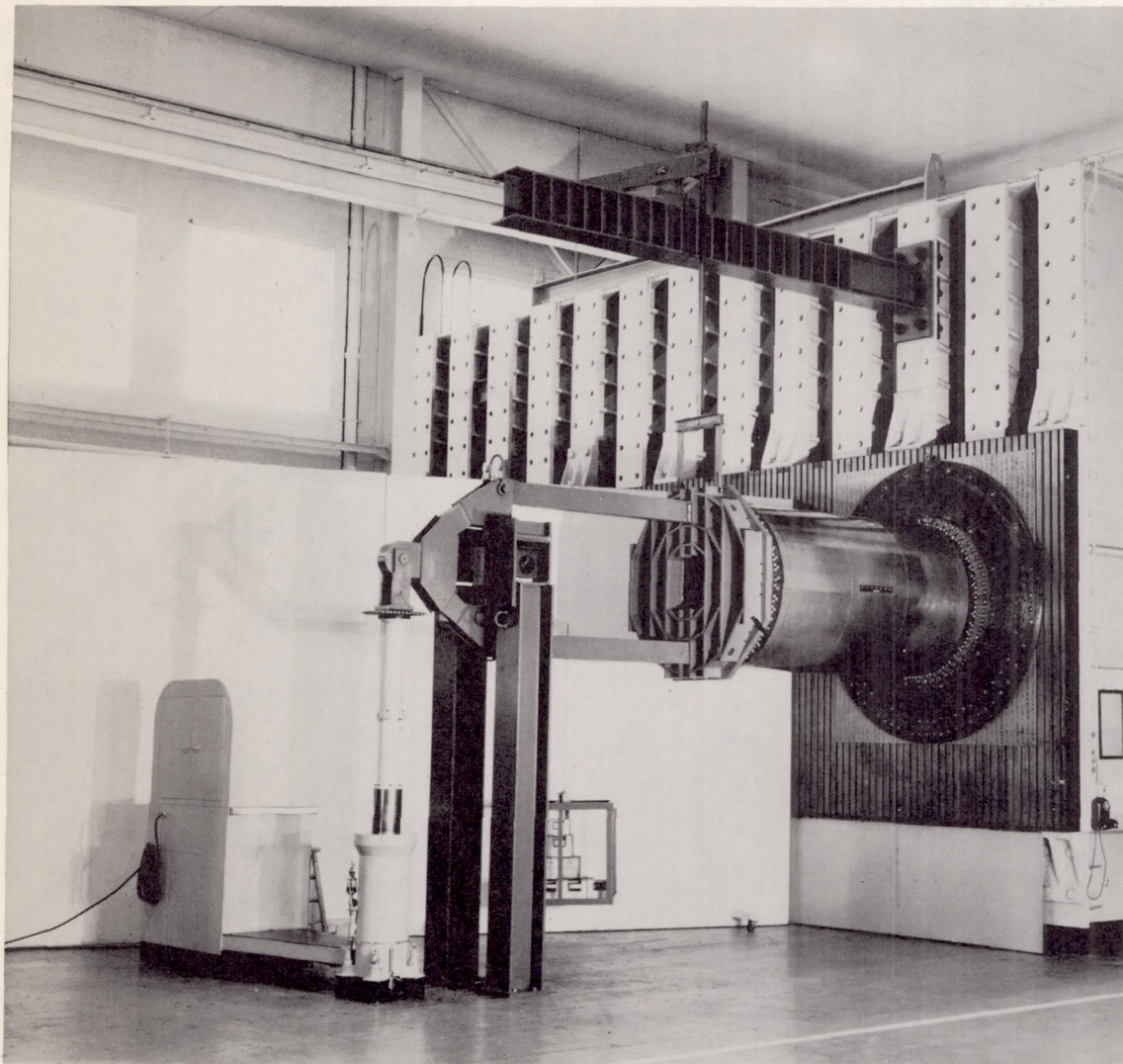
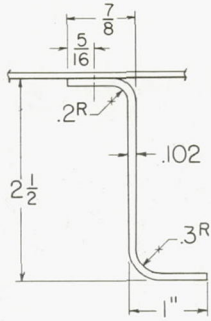
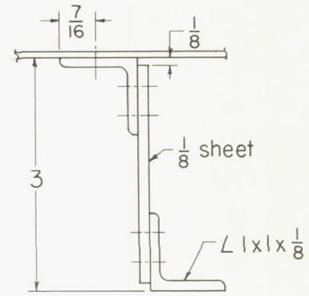


Figure 1.- Test setup.

L-87076



19- and 30-inch-diameter cylinders



48- and 77-inch-diameter cylinders

Figure 2.- Ring dimensions.

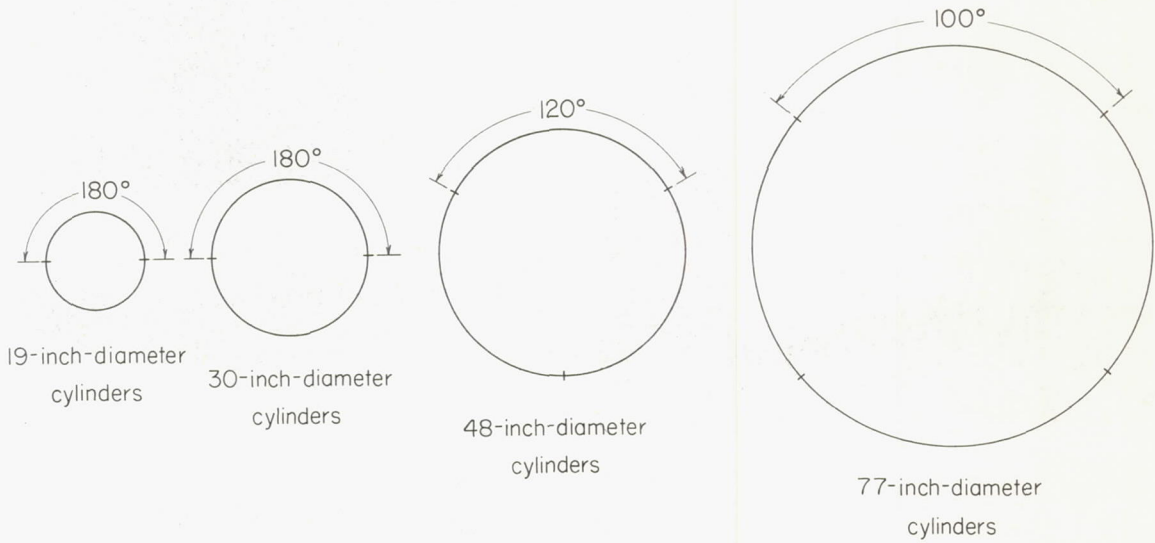
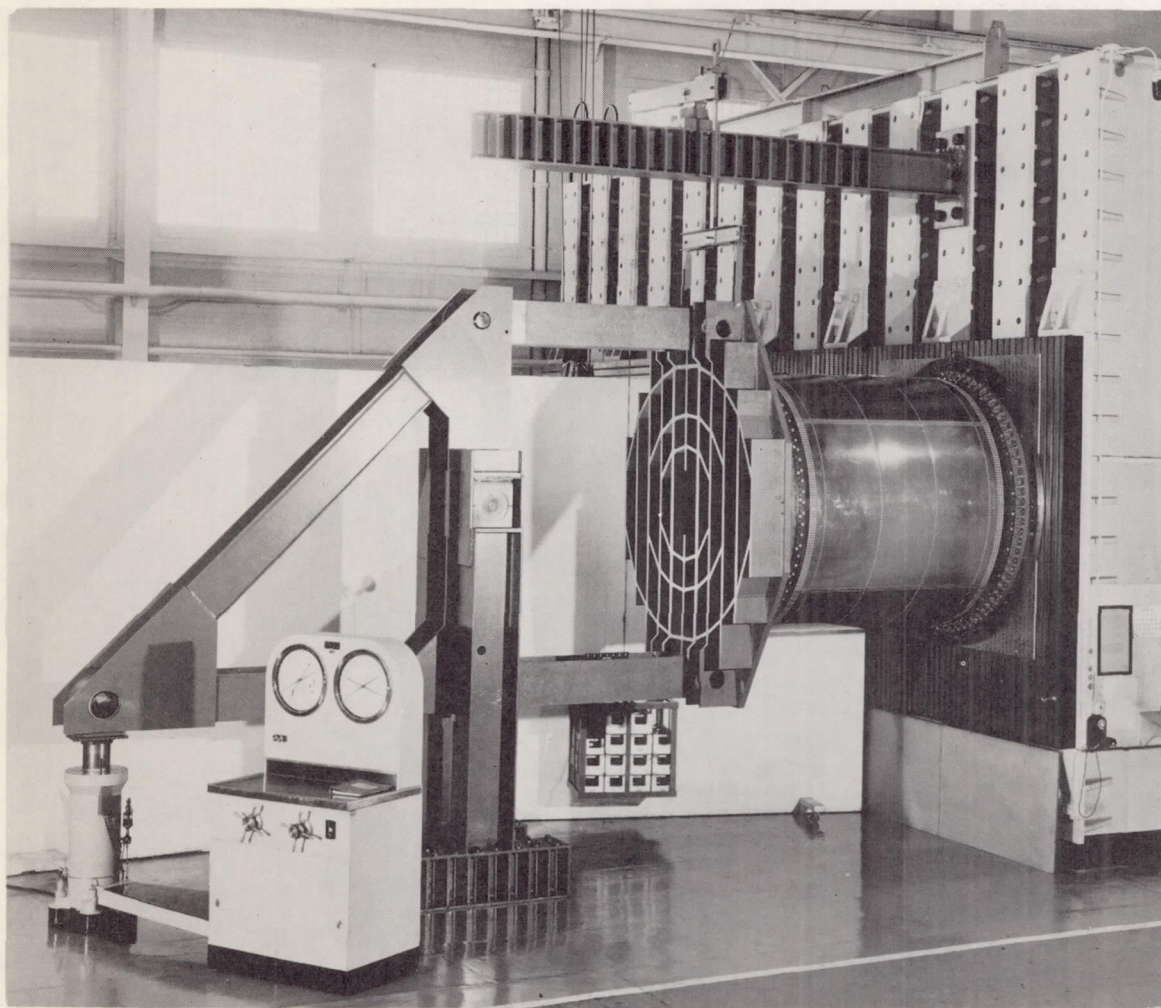


Figure 3.- Sheet splices on test cylinders.



L-88477

Figure 4.- Test setup for bending tests of cylinders of higher strength.

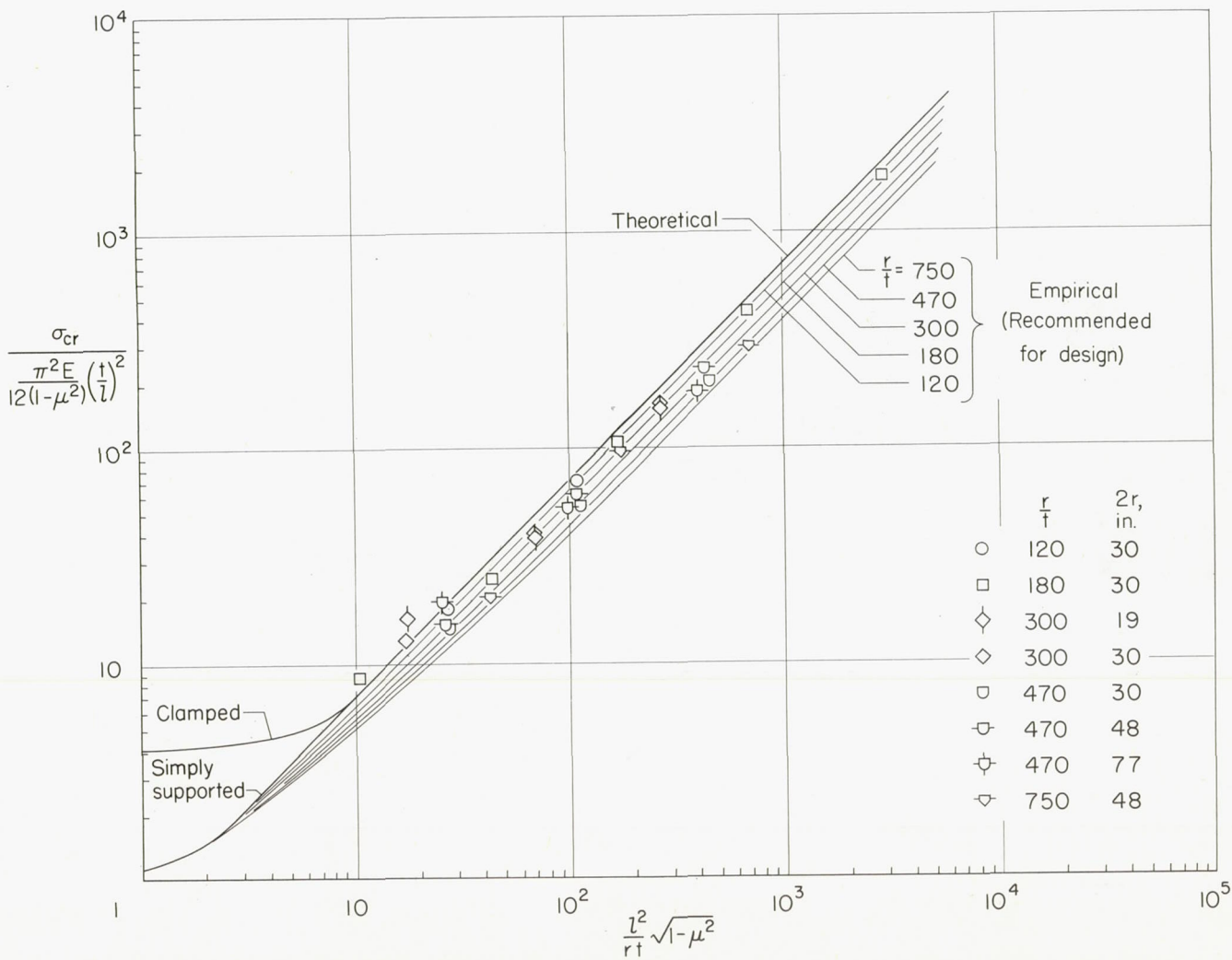


Figure 5.- Nondimensional plot of test data for cylinders in bending.  
The theoretical curve applies to cylinders in axial compression.

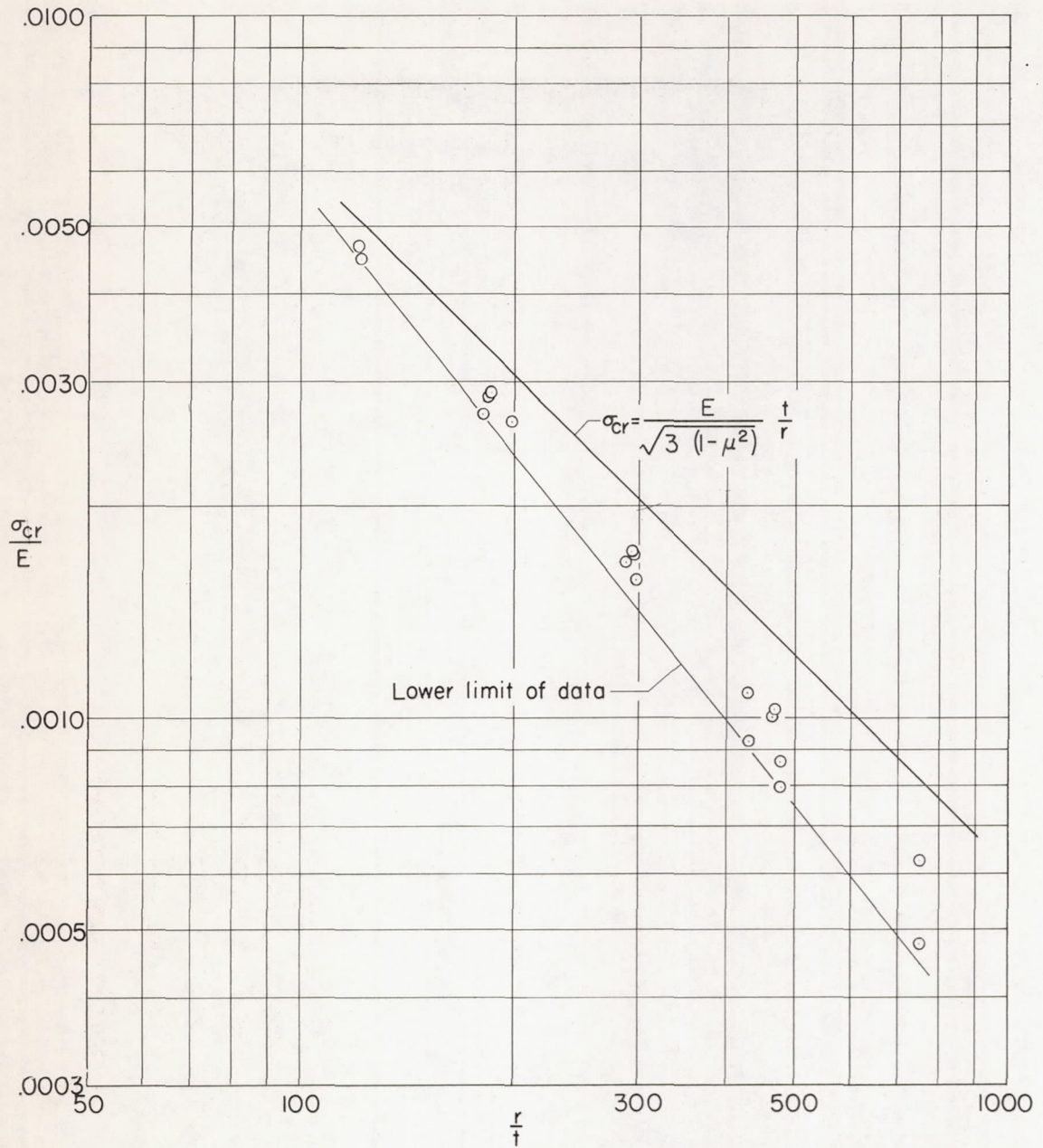


Figure 6.- Auxiliary plot of data from those cylinders with a ring-spacing-radius ratio greater than about 1/2.

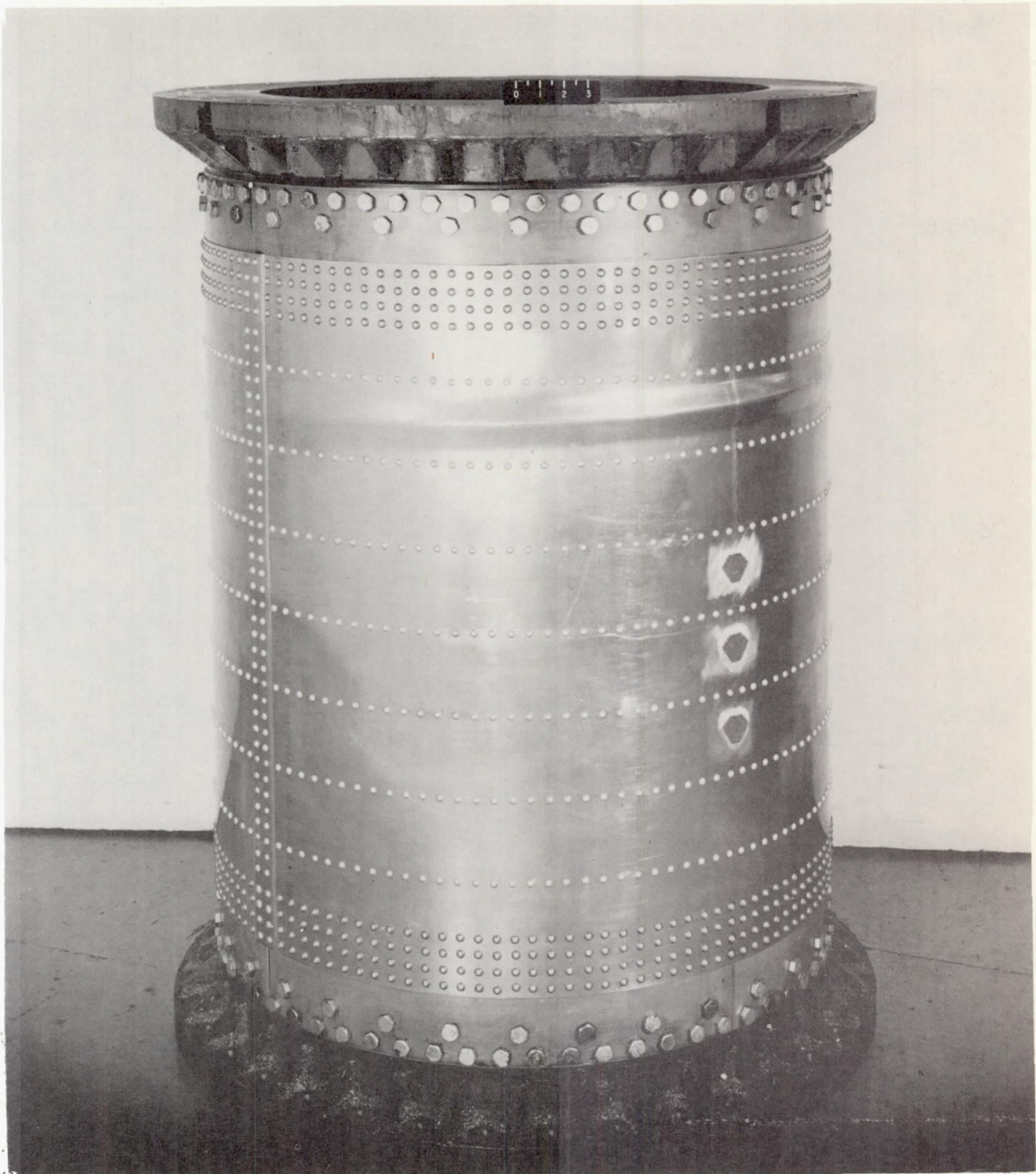


Figure 7.- Failure of cylinder 10.

L-89649